



Modification of optical and structural properties of DC magnetron sputtered tungsten oxide thin films for electrochromic application

Phasin YAEMSANGUANSAK^{1,*}, Manas SITTISHOKTRAM¹, Rungroj TUAYJAROEN¹, Ekkaphop KETSOMBUN¹, Tossaporn LERTVANITHPHOL², Chumphon LUANGCHAI SRI¹ and Tula JUTAROSAGA¹

¹Thin Film Technology Research Laboratory, Department of Physics, Faculty of Science, King Mongkut's University of Technology Thonburi, Pracha Uthit Rd., Bangkok, 10140, Thailand

²National Electronics and Computer Technology Center, National Science and Technology Development Agency (NSTDA), Pathum Thani, 12120, Thailand

*Corresponding author e-mail: phasin.yaemsanguansak@mail.kmutt.ac.th

Received date:

13 August 2018

Revised date:

18 February 2019

Accepted date:

23 March 2019

Keywords:

Electrochromic
Tungsten oxide
Reactive DC magnetron
sputtering

Abstract

The optical properties of tungsten oxide thin films prepared by a reactive DC magnetron sputtering technique were investigated. The influences of O₂ flow rates (15 and 18 sccm) and DC sputtering powers (5, 15 and 25 W) on the optical properties of 200 nm-thick tungsten oxide films on indium tin oxide substrates (WO₃/ITO/glass) were investigated using UV-visible spectrophotometer. The results indicated that the transmission modulation in visible region between colored state and bleached state of the films increased significantly with decreasing DC sputtering power and increasing O₂ flow rate. The results corresponded with the increase of film roughness and density which promoted the intercalation and deintercalation. The diffusion coefficient of the films was extracted from anodic peak current of cyclic voltammogram to determine the charge intercalation across the films. With the deposition power of 5 W and the O₂ flow rate of 18 sccm, the films showed the highest transmission modulation and differential optical density in visible region of 23.35% and 0.223, respectively. This information provided an advantage for developing high performance of electrochromic devices.

1. Introduction

Tungsten oxide has been studied for decades because its unique properties regarding a variety of optical-electrical properties such as electrochromism, photochromism, gas sensing and photocatalysis [1]. Reversible electrochromic color between bleached state and colored state is exploited intensively in electrochromic applications such as smart window for uses in buildings and automobiles, ski goggles, visor for motorcycle helmets [2], variable reflectance mirror and display devices [1]. Tungsten oxide is the most common for electrochromic devices because it is a superior inorganic electrochromic material regarding coloration efficiency and cyclic durability [1]. It has been prepared using various methods such as electrodeposition [3,4,5], sputtering [1,6,7,8,9,10], evaporation [11,12,13], chemical vapor deposition [14,15,16] and spray pyrolysis [17,18,19]. The coloration of tungsten oxide films is explained by the formation of tungsten bronze by the double injection of cations and electrons into the films using electric field. During the electrochromic process, intercalation and deintercalation of cations and electrons changes the optical properties of films at the colored state and bleached state. The electrochromic phenomenon of tungsten oxide can be expressed by the following equation: $WO_3 + xM^+ + xe^- \rightleftharpoons M_xWO_3$ where M⁺ is the cation such as H, Li, Na, K etc. [1].

As reported in the previous studies, the crystal structure, the oxygen and tungsten content in tungsten oxide films, film density and porosity showed key

roles in controlling the intercalation and deintercalation process causing the change of coloration efficiency of tungsten oxide films [6,20]. Therefore, in this study, a systematic attempt to adjust structural and optical properties was conducted by varying oxygen flow rates and sputtering powers of DC-magnetron sputtered tungsten oxide films. The oxygen flow rate was varied at 3, 6, 9, 12, 15 and 18 sccm and deposition power was varied at 5, 15 and 25 W. The tungsten oxide films prepared at appropriate deposition conditions with high differential optical density can be a potential material for developing high performance electrochromic application.

2. Experimental

2.1 Sample preparation

Oxygen partial pressures and sputtering power densities had showed the significant effects on the film quality [9,21,22]. Therefore, to control the film quality in the sputtering system, oxygen gas flow rates and sputtering powers had been varied. The deposited tungsten oxide thin films were prepared by reactive DC magnetron sputtering from a metallic tungsten target (3 inches and 99.99% purity). Deposition was operated under based pressure of 10⁻⁶ mbar with 3 sccm of Ar (99.99% purity) flow rate at room temperature. High purity O₂ gas (99.99% purity) was employed as reactive gas with the flow rates of 3, 6, 9, 12, 15 and 18 sccm. The oxygen partial pressure (P_{O₂})

was then calculated and varied from about 1×10^{-3} mbar to about 2.75×10^{-3} mbar. The sputtering power was set at 5, 15 and 25 W corresponding to the power density of 0.11, 0.33 and 0.55 W/cm². The films were deposited on indium tin oxide (ITO) coated on

borosilicate glass substrates and silicon wafers. The thickness was controlled using quartz thickness monitor about 200 nm. The deposition conditions including the deposition rate were listed in Table 1.

Table 1. Deposition conditions for WO₃ films.

O ₂ flow rate (sccm)	Power (W)	Working pressure ($\times 10^{-3}$ mbar)	P _{O₂} ($\times 10^{-3}$ mbar)	Power density (W/cm ²)	Deposition rate (angstrom·s ⁻¹)
	5	3.12	2.60	0.110	0.38 ± 0.07
15	15	2.96	2.47	0.329	1.22 ± 0.22
	25	2.96	2.47	0.548	1.68 ± 0.16
18	5	3.21	2.75	0.110	0.32 ± 0.04
	15	3.12	2.67	0.329	0.88 ± 0.08
	25	3.09	2.65	0.548	1.56 ± 0.16

2.2 Characterization

The preliminary optical properties were visually observed. While the transmission spectra of the films were studied using Halo vis-20 visible spectrophotometer. Surface morphology and RMS roughness of the films were obtained by scanning electron microscope (SEM, FEI Nova Nano SEM) operated at 5 kV and atomic force microscope (AFM, Bruker icon) with ScanAsyst mode. AFM images were characterized using WSxM 4.0 Beta 8.5 software. The elemental composition of films was analyzed by an energy dispersion spectrometer (EDS) equipped on SEM. The crystallographic and structure of the films were carried out from X-ray diffraction pattern measured using x-ray diffractometer (XRD, Bruker AXS). The refractive index was measured by ellipsometry technique (J.A. Woollam VASE 2000) and analyzed using Wvase 32. The relative film density was calculated through Lorentz-Lorenz relation based on the obtained refractive index.

The films were colored and bleached using electrochemical technique to determine transmission modulation and differential optical density (ΔOD). The sputtered films were used as the cathode and the Cu foil was used as the anode. The electrode potential was adjusted to -1.5 V for 60 s for colored state and then switched to +1.5 V for another 60 s for bleached state in 0.1 M HCl electrolyte solution. In addition, the electrochemical properties were evaluated based on the cyclic voltammograms (VersaSTAT 4 Potentiostat Galvanostat). The potential range and electrolyte solution were similar to the colored and bleached experiment with a scan rate of 50 mV·s⁻¹. The counter electrode and the reference electrode were Pt and Ag/AgCl, respectively. Finally, the diffusion coefficient was extracted and reported.

3. Results and discussion

3.1 Optical properties of bleached and colored as-deposited tungsten oxide films

Figure 1 showed the photographs of as-deposited films on the ITO/glass substrates at various oxygen

flow rates (3 - 12 sccm) and sputtering powers (5 - 25 W). The photographs showed that the as-deposited films at the oxygen flow rate of 3 sccm had gray and dark blue colors for all sputtering powers of 5, 15 and 25 W and tended to be darker with increasing sputtering power.

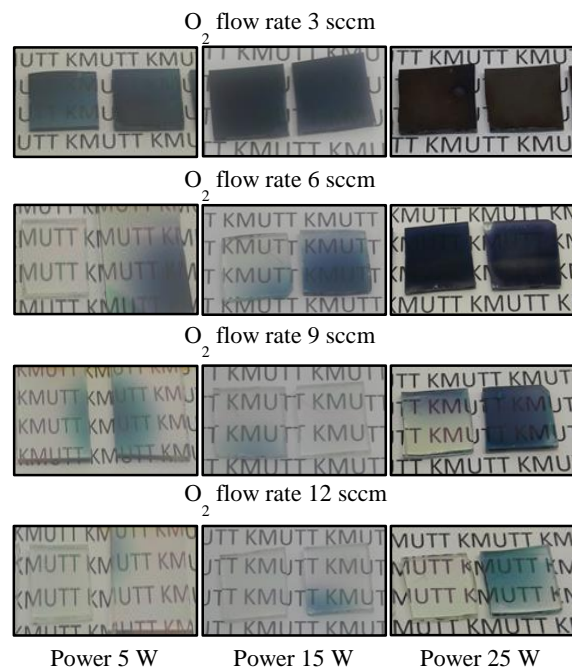


Figure 1. As-deposited WO₃ films with O₂ flow rate 3, 6, 9 and 12 sccm and sputtering power 5, 15 and 25 W.

The color started to become clear as the oxygen flow rates increased. At the power of 5 W, the film's color changed to light blue and clear starting at the oxygen flow rate of 6 sccm. While at the power of 15 and 25 W, the film changed from opaque to clear films at the oxygen flow rate of about 9 and 12 sccm, respectively. The opaque film at lower oxygen flow rate was possibly due to insufficient oxygen atoms incorporated into the films [23]. For the as-deposited films at 25 W with the oxygen gas flow rate of 3 sccm, the opaque films showed metal-like properties whose resistance can be easily measured. When the oxygen

gas flow rate increased to 15 and 18 sccm, the films (not shown here) were clear. Therefore, the focus of this study was at these oxygen gas flow rates with sputtering powers of 5, 15 and 25 W.

Figure 2. showed the transmission spectra of tungsten oxide films deposited with the O₂ flow rates of 15 and 18 sccm under the variation of sputtering powers of 5, 15, and 25 W at colored state and bleached state with the scan range from 320 to 1100 nm. For both O₂ flow rates, the transmittance in bleached state of tungsten oxide films changed slightly with increasing sputtering power from 5 to 25 W.

However, the transmittance in colored state of tungsten oxide films significantly increased as the sputtering power increased. Therefore, the colored state was suggested to be the key factor controlling the transmission modulation (the difference of transmittance between the colored and bleached states). In addition, the increase of O₂ flow rate with a constant sputtering power led to the increase of transmission modulation of tungsten oxide films. The results indicated that the film with low sputtering power of 5 W and high O₂ flow rate of 18 sccm displayed the highest transmission modulation.

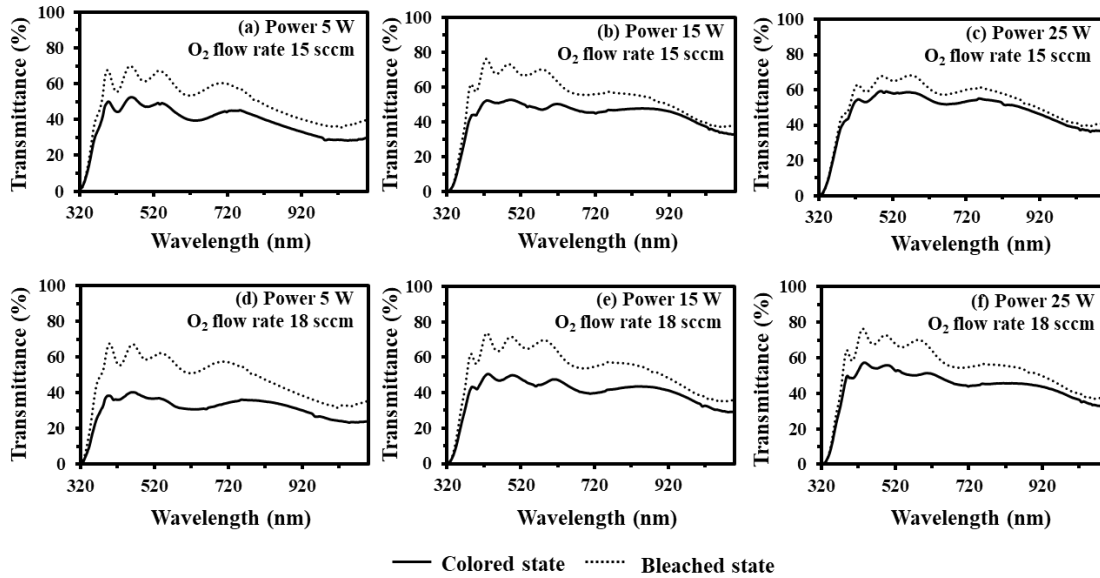


Figure 2. Transmission spectra of WO₃ films with the O₂ flow rate of 15 sccm and the sputtering powers of (a) 5, (b) 15 and (c) 25W and those with the O₂ flow rate of 18 sccm and the sputtering powers of (d) 5, (e) 15 and (f) 25W at colored state and bleached state.

For the quantification of transmission modulation, the average transmittance of the films in visible region was calculated and shown in Table 2. In the bleached state, the films with the oxygen flow rate of 15 sccm and the powers of 5, 15 and 25 W exhibited the transmittance (T_b) in visible region of 60.75, 66.05 and 62.15%, the films with the oxygen flow rate of 18 sccm and the powers of 5, 15 and 25 W exhibited the transmittance in visible region of 58.24, 64.22 and 65.58%, respectively. In the colored state, the films with the oxygen flow rate of 15 sccm and the powers of 5, 15 and 25 W showed the transmittance (T_c) in visible region of 45.27, 49.51 and 55.46%, the films with oxygen flow rate of 18 sccm and the power of 5, 15 and 25 W showed the transmittance in visible region of 34.89, 45.80 and 51.41%, respectively.

The differential optical density (ΔOD) was then calculated from the average transmission ratio between the bleached and colored states using the following equation.

$$\Delta OD = \log \frac{T_b}{T_c} \quad (1)$$

T_b and T_c are the average transmittance of the films in visible region at bleached and colored states. The data are illustrated in Table 2. The ΔOD of the samples increased with decreasing sputtering power and increasing oxygen flow rate. From these results, the highest ΔOD of 0.223 was obtained at the oxygen flow rate of 18 sccm and the power of 5 W. As mentioned previously that the colored state of tungsten oxide film with a low sputtering power controlled the transmission modulation. Since the colored states involved with the intercalation and deintercalation process, the film properties must promote these phenomena. According to Table 2, it was found that the ΔOD corresponded with the changes of surface roughness and film density. We then believed that these two parameters played important roles in enhancing the intercalation and deintercalation of the ions and electrons into the films [7,8].

Table 2. The transmittance at bleached (T_b) and colored (T_c) states, differential optical density (ΔOD) in visible region, RMS roughness, O/W ratio, relative density and diffusion coefficient of WO_3 films.

O ₂ flow rate (sccm)	Power (W)	T _b (%)	T _c (%)	ΔOD	RMS roughness (nm)	O:W	Relative density	Diffusion coefficient ($\times 10^{-10} \text{ m}^2\cdot\text{s}^{-1}$)
15	5	60.75	45.27	0.128	3.10 ± 0.18	3.50	0.872	18.92
	15	66.05	49.51	0.125	2.33 ± 0.08	3.45	0.867	35.90
	25	62.15	55.46	0.049	2.33 ± 0.15	3.53	0.863	42.17
18	5	58.24	34.89	0.223	3.09 ± 0.15	3.70	0.867	57.81
	15	64.22	45.80	0.147	2.58 ± 0.37	3.33	0.866	22.73
	25	65.58	51.41	0.106	2.92 ± 0.18	3.42	0.864	53.82

3.2 Physical properties of as-deposited tungsten oxide films

This section is devoted to describe the physical properties including the morphology, RMS roughness, relative film density, chemical content and structure of as-deposited tungsten oxide films. The SEM micrographs of as-deposited WO_3 /ITO/glass substrate with various conditions are shown in Figure 3. The SEM and AFM measurements reviewed that the surface of tungsten oxide film with the O_2 flow rate of 15 sccm and the power of 5 W consisted of the large grain sizes with 3.10 ± 0.18 nm of RMS roughness. Figure 3(b) showed the SEM image of tungsten oxide film with the O_2 flow rate of 15 sccm and the power of 15 W. The surface showed high roughness with small grain sizes and pores. The RMS roughness decreased to 2.33 ± 0.08 nm due to the increase of sputtering power. Figure 3(c) showed the SEM of WO_3 with the O_2 flow rate of 15 sccm and the power of 25 W, the surface morphology of tungsten oxide film was quite smooth with the RMS roughness of 2.33 ± 0.15 nm. From the results, it indicated that the roughness of the WO_3 films decreased with increasing sputtering

power. Typically, the mobility improvement of adatoms on the substrate surface is required to form a smooth surface. It is believed that the high DC sputtering power in magnetron sputtering system energizes inert argon gas by momentum transfer process. These adatoms with sufficient kinetic energy then enhanced the surface diffusion and the nucleation to form smooth film surface [24].

Figures 3(d), (e) and (f) showed the SEM of tungsten oxide films with the O_2 flow rate of 18 sccm, the morphology of these conditions with increasing sputtering power looked similar to the films deposited under the O_2 flow rate of 15 sccm. The roughness of the films decreased from 3.09 ± 0.15 to 2.92 ± 0.18 nm with increasing sputtering power. Comparing the RMS roughness of the samples between the O_2 flow rate of 15 sccm and 18 sccm, the RMS roughness of the films increased at the same operation power. Except at the power of 5 W, the films deposited with both O_2 flow rate showed the similar value of RMS roughness. The increasing O_2 flow rate could increase the working pressure during deposition process which causes the rough surface morphology [25].

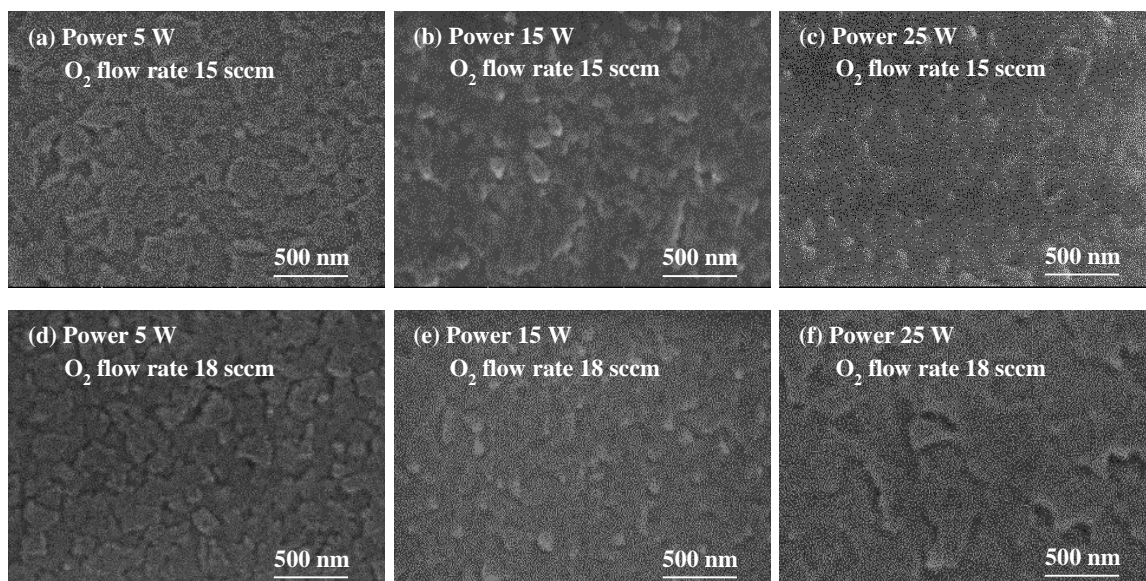


Figure 3. Surface SEM micrographs of WO_3 with the O_2 flow rate of 15 sccm and the sputtering powers of (a) 5, (b) 15 and (c) 25W and those with the O_2 flow rate of 18 sccm and the sputtering powers of (d) 5, (e) 15 and (f) 25W.

The refractive index at 550 nm of as-deposited tungsten oxide on silicon wafers was measured using the spectroscopic ellipsometry technique. Then the relative densities were calculated based on the obtained refractive index using the Lorentz – Lorentz relation according to the following equations [7, 8].

$$P = \left(\frac{\rho_f}{\rho_b}\right) = \left(\frac{n_f^2-1}{n_f^2+2}\right) \left(\frac{n_b^2+2}{n_b^2-1}\right) \quad (2)$$

P is a relative density of tungsten oxide film, ρ_f and ρ_b are density of tungsten oxide film and bulk, respectively. n_f and n_b are refractive indices of film and bulk material at 550 nm ($n_b = 2.5$). According to Table 2, as the sputter power increased from 5, 15 to 25 W, the relative density of tungsten films decreased from 0.876, 0.867 to 0.863 for the specimens with the oxygen flow rate of 15 sccm and 0.867, 0.866 to 0.864 for those with the oxygen flowrate of 18 sccm, respectively. The decrease of relative density showed the correlation with the deposition rate. As the deposition rate increased (Table 1.) according to the increase of sputtering power, sputtered atoms from the target quickly reached the substrates. There was not sufficient time for the atomic arrangement causing the decrease of relative density. While, lower deposition rate showed higher relative film density.

The increase of oxygen flow rate increased the total pressure of the system causing the shorter mean free path of sputtered atoms which lowered the energy of the sputtered atoms for the arrangement at the substrates. The increase of oxygen partial pressure had a similar effect to the increase of total pressure reported by [26] causing the reduction of the deposition rate as shown in Table 1. In addition, the decrease of relative film density could also be related to the percentage of oxygen atoms within the films. However, in our case, the ratio of oxygen to tungsten did not change significantly. Therefore, lower energy of sputtered atoms was suggested to be the main effect of lowering the film density.

Tungsten oxide films deposited at a constant O_2 flow rate showed that the increase of sputtering power led to both relative density and ΔOD decreased. From this result, it indicated that ΔOD decreased proportionally with relative density reduction. The insufficient density of tungsten oxide molecules would decrease the performance of colored state of films due to low concentration of tungsten bronze during coloration of electrochromic reaction.

The elemental analysis of WO_3 films was studied using EDS. Figure 4 showed the EDS spectrum of WO_3 film with the O_2 flow rate of 18 sccm and the sputtering power of 5 W. The analysis of EDS spectra confirmed the presence of W and O in the films. The obtained O/W ratios were listed in Table 2. Tungsten oxide films sputtered with various sputtering powers and 15 sccm of O_2 flow rate showed small variation of O/W ratio which insignificantly affected the differential optical density. In addition, the films sputtered with O_2 flow rate of 18 sccm showed a large

variation of O/W ratio as sputtering power changed. However, tungsten oxide films deposited at 18 sccm of O_2 flow rate and 5 W of sputtering power with the highest O/W ratio showed the highest ΔOD . The higher of O/W ratio with appropriate stoichiometry might permit the generation of H^+W^{5+} states (tungsten bronze) and relatively lower trapping of charges which promoted the electrochromic efficiency. [27]. It indicated that tungsten oxide films with optimal oxygen concentration was favorable to increase ΔOD . [28]

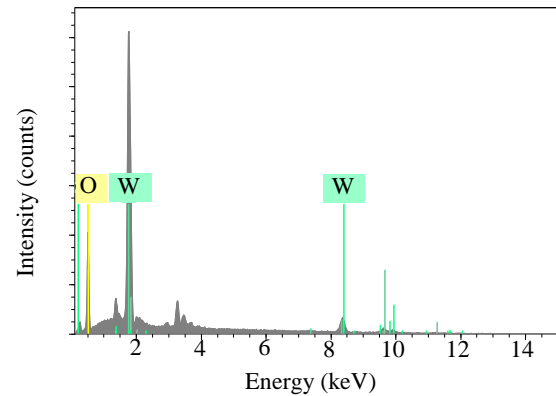


Figure 4. EDS spectrum of an as-deposited WO_3 film with the O_2 flow rate of 18 sccm and the sputtering power of 5W.

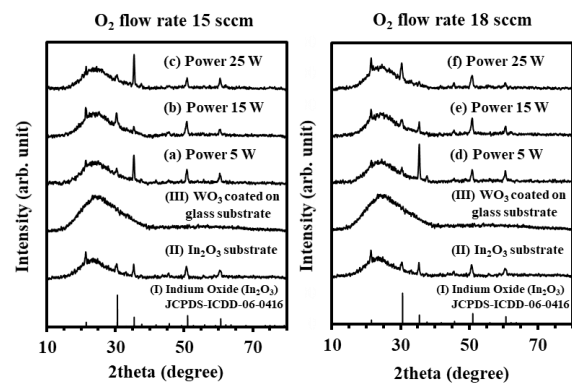


Figure 5. XRD pattern of WO_3 films with various sputtering powers and O_2 flow rates.

Figure 5 showed XRD patterns of WO_3 films deposited on ITO/glass substrate at O_2 flow rate 15 and 18 sccm and sputtering powers of 5, 15 and 25 W. It clearly showed that all films were amorphous because no diffraction peak of WO_3 were observed except the diffraction peaks of the ITO substrate. As shown in Figure 5, when compared the XRD spectra of 200-nm WO_3 /ITO/glass with that of 200-nm WO_3 /glass, the broad peak of the glass without remarkable XRD peaks of WO_3 films was also observed.

The ions and electrons injected into WO_3 films cause the color change. The process is faster in amorphous films than crystalline films due to lower density of amorphous films [29]. The orderly structure of atoms in crystalline structure would not favor the

intercalation and deintercalation of the charges into the films. The diffraction patterns indicate an amorphous structure which is usually a feature of the films prepared by sputtering deposition at room temperature [30].

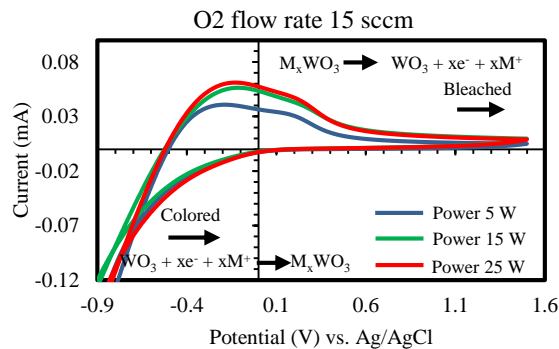


Figure 6. Cyclic voltammograms (third cycle) of WO_3 films with O_2 flow rate 15 sccm at different sputtering powers.

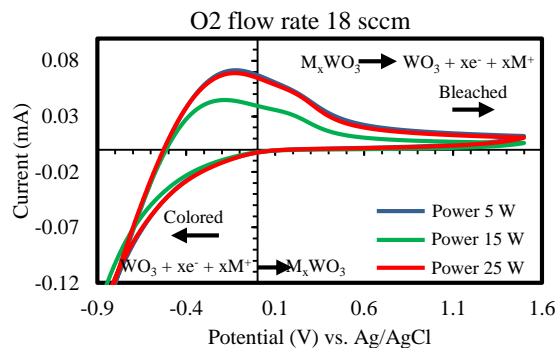


Figure 7. Cyclic voltammograms (third cycle) of WO_3 films with O_2 flow rate 18 sccm at different sputtering powers.

3.3 Electrochromic properties of tungsten oxide films

Figures 6 and 7 showed the cyclic voltammograms of tungsten oxide films with O_2 flow rates of 15 and 18 sccm and sputtering powers of 5, 15 and 25 W. The anodic peak current of the samples was utilized to calculate diffusion coefficient which were used to analyze intercalation and deintercalation of cations and electrons across the films in electrochromic process. The diffusion coefficient was calculated as following equation [31].

$$i_p = (2.69 \times 10^5) \times n^{3/2} \times A \times C \times D^{1/2} \times V^{1/2} \quad (3)$$

where i_p is the peak anodic current (A), $n = 1$ is number of electrons involved in the process, A is area of electrode (m^2), C is solution concentration (mol m^{-3}), D is diffusion coefficient ($\text{m}^2 \text{s}^{-1}$), V is scan rate (V s^{-1}) and 2.69×10^5 is constant in the unit of $\text{A s V}^{-1/2}$. The anodic peak current and diffusion coefficient of tungsten oxide films with O_2 flow rate of 15 sccm increased with increasing sputtering power from 5 to 25 W as shown in Table 2. The increase of diffusion coefficient could also be the results of the decrease of relative density which corresponded to the increase of charge mobility in intercalation process.

Tungsten oxide films with 18 sccm of O_2 flow rate showed the decrease of diffusion coefficient when the sputtering power increased from 5 W to 15 W then it

increased again when the sputtering power increased to 25 W. In this part, the diffusion coefficient was not related to the relative density which might occur from film surface roughness. Normally, the diffusion coefficient presented the diffusion transport of charges into the films for injection/ejection in electrochromic process which would affect ΔOD . However, the diffusion coefficient was not related to ΔOD in our experiment because there was an effect from the surface roughness. The films with higher RMS roughness exhibited high surface area for electrochromic reaction which facilitated charges intercalation and led to increase in diffusion coefficient.

4. Conclusions

In conclusion, the optical properties of tungsten oxide films can be tuned by the modification of oxygen flow rate and sputtering power using reactive dc magnetron sputtering. The differential optical density of the films was enhanced by the increase of film density and roughness corresponding to the decrease of sputtering power and the increase of oxygen flow rate. The obtained amorphous structure and high RMS roughness with high diffusion coefficient would facilitate the intercalation and deintercalation of ions and electrons for the enhancement of the electrochromic and optical properties. In this experiment, the highest differential optical density and diffusion coefficient of 0.223 and $57.81 \times 10^{-10} \text{ m}^2 \cdot \text{s}^{-1}$ were obtained at the oxygen flow rate of 18 sccm and the power of 5 W. These films have potential for developing high performance electrochromic devices.

5. Acknowledgements

The authors gratefully to acknowledge the financial support provided by the Thin Film Technology Research Laboratory, Department of Physics, Faculty of Science of King Mongkut's University Technology of Thonburi.

References

- [1] K. Nakagawa, N. Miura, S. Matsumoto, R. Nakano and H. Matsumoto, "Electrochromism and Electronic Structures of Nitrogen Doped Tungsten Oxide Thin Films Prepared by RF Reactive Sputtering," *Japanese Journal of Applied Physics*, vol. 47, pp. 7230-7235, 2008.
- [2] G. A. Niklasson, and C. G. Granqvist, "Electrochromics for smart windows: thin films of tungsten oxide and nickel oxide, and devices based on these," *Journal Materials Chemistry*, vol. 17, pp. 127-156, 2007.
- [3] J. C. Chou, P. A. Ho, C. J. Yang and Y. H. Liao, "Photoelectric Characteristics and Equivalent Circuit Analysis of Flexible Tungsten Oxide Electrochromic Thin Film," *Journal of Display Technology*, vol. 10, pp. 821-826, 2014.

- [4] G. F. Cai, D. Zhou, Q. Q. Xiong, J. H. Zhang, X. L. Wang, C.D. Gu and J. P. Tu, "Efficient electrochromic materials based on TiO₂@WO₃ core/shell nanorod arrays," *Solar Energy Materials and Solar Cells*, vol. 117, pp.231-238, 2013.
- [5] H. M. A. Soliman, A. B. Kashyout, M. S. E. Nouby and A. M. Aboeshly, "Preparation and characterizations of tungsten oxide electrochromic nanomaterials," *Journal of Materials Science: Materials in Electronics*, vol. 21, pp. 1313-1321, 2010.
- [6] C. Brigouleix, P. Topart, E. Bruneton, F. Sabary, G. Nouhaut and G. Campet, "Roll-to-roll pulsed de magnetron sputtering deposition of WO₃ for electrochromic windows," *Electrochimica Acta*, vol. 46, pp. 1931-1936, 2001.
- [7] X. Sun, Z. Liu and H. Cao, "Electrochromic properties of N-doped tungsten oxide thin films prepared by reactive DC-pulsed sputtering," *Thin Solid Films*, vol. 519, pp. 3032-3036, 2011.
- [8] E. Washizu, A. Yamamoto, Y. Abe, M. Kawamura and K. Sasaki, "Optical and electrochromic properties of RF reactively sputtered WO₃ films," *Solid State Ionics*, vol. 165, pp. 175-180, 2003.
- [9] A. Subrahmanyam and A. Karuppasamy, "Optical and electrochromic properties of oxygen sputtered tungsten oxide (WO₃) thin films." *Solar Energy Materials and Solar Cells*, vol. 91, pp. 266-274, 2007.
- [10] Y. S. Lin, Y. L. Chiang and J. Y. Lai, "Effects of oxygen addition to the electrochromic properties of WO_{3-z} thin films sputtered on flexible PET/ITO substrates," *Solid State Ionics*, vol. 180, pp. 99-105, 2009.
- [11] P. Losier and P. V. Ashrit, "Flash evaporated tungsten oxide thin films for electrochromic applications," *Journal of Materials Science Letters*, vol. 22, pp. 1095-1098, 2003.
- [12] A. Lusic, J. Kleperis and E. Pentjuss, "Model of electrochromic and related phenomena in tungsten oxide thin films," *Journal of Solid State Electrochemistry*, vol. 7, pp. 106-112, 2003.
- [13] E. Ozkan, S. H. Lee, C. E. Tracy, J. R. Pitts and S. K. Deb, "Comparison of electrochromic amorphous and crystalline tungsten oxide films," *Solar Energy Materials and Solar Cells*, vol. 79, pp. 439-448, 2003.
- [14] H. C. Chen, D. J. Jan, C. H. Chen and K. T. Huang, "Bond and electrochromic properties of WO₃ films deposited with horizontal DC, pulsed DC, and RF sputtering," *Electrochimica Acta*, vol. 93, pp. 307-313, 2013.
- [15] K. Gesheva, A. Szekeres and T. Ivanova, "Optical properties of chemical vapor deposited thin films of molybdenum and tungsten based metal oxides," *Solar Energy Materials and Solar Cells*, vol. 76, pp. 563-576, 2003.
- [16] J. Scarminio, M. A. Bica de Moraes, R. C. E. Dias, F. P. Rouxinol and S. F. Durrant, "tungsten oxide films of high electrochromic efficiencies obtained by deposition," *Electrochemical and Solid-State Letters*, vol. 6, pp. H9-H12, 2003.
- [17] P. S. Patil, "Solution thermolysed tungsten oxide-based electrochromic devices: thickness-dependent step potential analysis," *Journal of Solid State Electrochemistry*, vol. 6, pp. 284-287, 2002.
- [18] M. Rezagui, M. Addou, A. Outzourhit, E. El Idrissi, A. Kachouane and A. Bougrine, "Electrochromic effect in WO₃ thin films prepared by spray pyrolysis," *Solar Energy Materials and Solar Cells*, vol. 77, pp. 341-350, 2003.
- [19] R. Sivakumar, A. M. E. Raj, B. Subramanian, M. Jayachandran, D. C. Trivendi and C. Sanjeeviraja, "Preparation and characterization of spray deposited n-type WO₃ thin films for electrochromic devices," *Materials Research Bulletin*, vol. 39, pp. 1479-1489, 2004.
- [20] T.-S. Yang, Z.-R. Lin and M.-S. Wong, "Structure and electrochromic properties of tungsten oxide films prepared by magnetron sputtering," *Applied Surface Science*, vol. 252, pp. 2029-2037, 2005.
- [21] X. Sun, Z. Liu and H. Cao, "Effect of films density on electrochromic tungsten oxide thin films deposited by reactive de-pulsed magnetron sputtering," *Journal of Alloys and Compounds*, vol. 504S, pp. S418-S421, 2010.
- [22] B. Liu, Q. H. L. Wen and X. Zhao, "The effect of sputtering power on the structure and photocatalytic activity of TiO₂ films prepared by magnetron sputtering," *Thin Solid Films*, vol. 517, pp. 6569-6575, 2009.
- [23] M. Weil and W.-D. Schubert, "The beautiful colors of tungsten oxides", in *International tungsten Industry Association*, 4 Heathfield Terrace, London, 2013, pp. 1-12.
- [24] M. T. Le, Y. U. Sohn, J. W. Lim and G. S. Choi, "Effect of sputtering power on the nucleation and growth of cu films deposited by magnetron sputtering," *Materials Transactions*, vol. 51, pp. 116-120, 2010.
- [25] N. Oka, M. Watanabe, K. Sugie, Y. Iwabuchi, H. Kotsubo and Y. Shigesato, "Reactive-gas-flow sputter deposition of amorphous WO₃ films for electrochromic devices," *Thin Solid Films*, vol. 532, pp. 1-6, 2013.
- [26] B. Baloukas, J.-M. Lamarre and L. Martinu, "Electrochromic interference filters fabricated from dense and porous tungsten oxide films," *Solar Energy Material and Solar Cells*, vol. 95, pp. 807-815, 2011.
- [27] A. Antonaia, T. Polichetti, M. L. Addonizio, S. Aprea, C. Minarini and A. Rubino, "Structure and optical characterization of amorphous and crystalline evaporated WO₃ layers," *Thin Solid Films*, vol. 354, pp. 73-81, 1999.

- [28] A. I. Inamdar, Y. S. Kim, B.U. Jang, H. Im, W. Jung, D.-Y. Kim and H. Kim, "Effects of oxygen stoichiometry on electrochromic properties in amorphous tungsten oxide films," *Thin Solid Films*, vol. 520, pp. 5367-5371, 2012.
- [29] P. M. S. Monk, R. J. Mortimer and D. R. Rosseinsky, *Electrochromism and Electrochromic Devices*. Cambridge University Press, 2007.
- [30] X. G. Wang, Y. S. Jiang, N. H. Yang, L. Yuan and S. J. Pang, "Crystallinity and morphology changes of α -WO₃ films," *Applied Surface Science*, vol. 143, pp. 135-141, 1999.
- [31] G. kreysa, K.-I. Ota and R. Savinell, *Encyclopedia of Applied Electrochemistry*. Springer New York Heidelberg Dordrecht London, 2014.